RSC Advances

PAPER

View Article Online
View Journal | View Issue

Cite this: *RSC Adv.*, 2025, **15**, 40491

Multi-stimulus responsive polyoxometalate–viologen hybrid ionic liquids for rewritable inkless printing and environmental monitoring

Hanfei Deng,[a] Simin Jia,[a] Yu Zhang,[a] Yuanyuan Zhang,[a] Jiang Shao,[b] Muhammad Wasim Afzal,[a] Xue Liu, *[a] Dongbin Dang *[a] and Yan Bai *[a]

Multi-stimulus responsive materials have attracted significant attention due to their ability to respond dynamically to multiple external stimuli, including light, temperature, and chemical signals. Achieving both rapid response times and precise selectivity is essential for advancing the functionality of such materials. In this study, five polyoxometalate-based viologen ionic liquids (ILs) were synthesized through ion exchange between $H_3PMo_{12}O_{40}$ and viologen ILs with varying substituents. These ILs demonstrated multi-stimulus responses to light and ammonia gas. Under Xe lamp irradiation, all ILs exhibited prominent photochromism, with C_{12}–PMo_{12} undergoing a rapid change from light yellow to light green within just 5 seconds. Exposure to an H_2O_2 atmosphere for 3 hours resulted in the complete decolorization of C_{12}–PMo_{12}. Remarkably, after five cycles of coloring and decoloring, its absorbance remained virtually unchanged, highlighting its excellent reversibility and stability. Additionally, as the alkyl chain length of the viologen-based cation increased, the coloring rate accelerated, and the color contrast enhanced, likely due to the suppression of viologen radical quenching by longer carbon chains. These ILs also exhibited gas-chromic behavior in the presence of ammonia, showing high detection selectivity. Furthermore, the materials were successfully applied in inkless erasable printing and ultraviolet detection. The C_{12}–PMo_{12}-based carbon paper displayed clear and readable prints in only 10 seconds and could be bleached in an H_2O_2 atmosphere within 1.5 hours. These findings demonstrate that the synthesized ILs possess versatile multi-stimulus responsive properties, making them highly promising for applications in inkless printing, ultraviolet detection, and amine vapor sensing.

Received 11th August 2025
Accepted 26th September 2025

DOI: 10.1039/d5ra05884h

rsc.li/rsc-advances

1. Introduction

To address the demands of an increasingly intelligent society, stimulus-responsive polymers[1,2] have garnered significant scientific interest for a wide range of applications,[3,4] particularly in the domain of stimulus-responsive color-changing materials.[5–9] These materials undergo color changes in response to external stimuli, such as light, temperature, gas, electricity, and pH, and hold considerable potential for applications in diverse areas, including information storage and encryption,[10,11] sensing,[12–14] and anti-counterfeiting.[15,16] Viologens exhibit excellent electron-accepting capabilities and possess Lewis acidic sites.[17–19] The electron-deficient viologen cation (V^{2+}) can undergo one-electron transfer from an appropriate electron donor to form the viologen cationic radical ($V^{\bullet+}$). A distinct color change typically accompanies this process. Consequently, viologens and their derivatives exhibit notable stimulus-responsive color-changing properties,[20–23] showing great promise in fields such as optical switching,[24] sensors,[25–27] anti-counterfeiting,[28,29] and inkless printing.[30,31] A significant challenge for viologen-based chromic materials is achieving quick response times and high stability. A practical approach to developing stable and rapid multi-stimulus responsive chromic materials is the incorporation of viologen derivatives into high-performance electron donors.

Polyoxometalates (POMs), known for their favorable redox properties and abundance of electrons,[32,33] are regarded as excellent electron donors. This makes them compatible with the electron-acceptor properties of viologens, facilitating efficient electron transfer.[34,35] Several noteworthy studies have been published on polyoxometalate–viologen hybrid chromic materials.[36–39] For instance, Zhang's group developed a new crystalline polyoxometalate–viologen hybrid,[40] which demonstrated remarkable ultraviolet light detection capabilities. The material exhibited an apparent color change from pale yellow to blue and a rapid response to ultraviolet light, with detection at intensities as low as 0.006 mW cm^{-2} in narrow-band UV regions. However, it can only maintain a longer duration in the dark, and as the light intensity increases, the exposed cations

[a]*Longzihu New Energy Laboratory, College of Chemistry and Molecular Sciences, Henan University, Kaifeng 475004, PR China. E-mail: xliu@henu.edu.cn*
[b]*School of Mechanical Engineering, Jiangsu University of Science and Technology, Zhenjiang 212100, P. R. China*

are easily oxidized, leading to a decrease in fluorescence intensity. Jun's group achieved fast-response photochromism by utilizing two types of viologen ligands,[41] resulting in the synthesis of three POM-based compounds under hydrothermal and solvothermal conditions. These compounds proved to be effective as visible UV detectors and inkless erasable printing materials, while the spectra of each element overlap before and after the XRS spectral test changes. Chen's group synthesized a thermochromic polyoxometalate-based metal–organic framework (POMOF) using Keggin-type polyoxometalates and metalloviologens,[42] which exhibited reversible color changes from yellow to black at 150 °C. Despite these advances, the development of novel multifunctional stimuli-responsive hybrid chromic materials remains a significant challenge. The above studies focus on maximizing and stabilizing color changes, while overlooking the difficulty of material reproducibility. The hard and brittle nature of metal framework structures, along with their poor solubility, limits their applications in flexible devices. Therefore, constructing multifunctional stimulus-responsive hybrid color-changing materials with fast response, long-term retention, and good flexibility remains a significant challenge.

Ionic liquids (ILs) are organic molten salts at room temperature, composed of organic cations and either organic or inorganic anions. These materials have garnered significant attention due to their wide electrochemical window, high ionic conductivity, and tunable structural properties. Polyoxometalate-based ionic liquids (POM-ILs) are organic–inorganic hybrid materials that combine various cations with polyoxometalate (POM) anions. These POM-ILs combine the unique characteristics of polyoxometalates and ionic liquids, and hold great promise for realizing multifunctional stimulus-responsive hybrid color-changing materials with fast response, long-term stability, and good flexibility.[43] In this study, five ionic liquids (C_n–PMo_{12}, where $n = 3, 4, 5, 6, 12$) were prepared using POMs with multi-electron donor characteristics as anions and 4,4′-bipyridine, which is prone to reversible redox reactions, as cations. The color-changing behavior of these five ILs in response to external stimuli, such as light and ammonia were also investigated. All five ILs exhibited rapid and noticeable photochromic behavior upon exposure to light. Remarkably, C_{12}–PMo_{12} demonstrated the most pronounced photochromism, transitioning from yellow to light green within 5 seconds. These ILs show significant potential for applications in inkless erasable printing and UV detection technologies. Furthermore, they also displayed discoloration when exposed to ammonia and organic amines, with high selectivity, suggesting their promising use as organic amine detectors.

2. Experimental

2.1. Materials and methods

Phosphoric acid (85 wt% in water solution), hydrochloric acid (36–38wt%), $Na_2WO_4 \cdot 2H_2O$ (purity, >99%), 4,4′-bipyridine, 1-bromopropane, 1-bromobutane, 1-bromopentane, 1-bromohexane, 1-bromodecane, acetone, *N*,*N*-dimethylformamide (DMF), ethanol and diethyl ether were all supplied by Aladdin Reagent Co., Ltd China. Polydimethylsiloxane (PDMS; SYLGARD® 184 elastomer) was purchased from Gelest Inc., USA. Proton nuclear magnetic resonance (^{1}H NMR) spectra were recorded on a Bruker 500 spectrometer at room temperature. FT-IR spectroscopy was performed using a VERTEX-70 spectrometer with a test range of 4000–400 cm^{-1}. PXRD patterns were generated using Bruker D8 Advance. The ultraviolet-visible (UV-vis) absorption spectra were obtained by making use of a UH4150 ultraviolet spectrophotometer at room temperature. Electron paramagnetic resonance (EPR) spectra were recorded at RT with a Bruker EMX PLUS apparatus. X-ray photoelectron spectroscopy (XPS) was performed using monochromatic radiation on the ESCALB250Xi spectrometer.

2.2. Syntheses and characterization

2.2.1. Preparation of viologen-based ionic liquid. As shown in Fig. 1, $C_n$bpy·Br (where $n = 3, 4, 5, 6, 12$) was synthesized following the method previously reported.[44] The successful synthesis was confirmed by the ^{1}H NMR spectrum, as presented in Fig. S1–S5.

2.2.2. Preparation of polyoxometalates-based ionic liquid. $H_3PMo_{12}O_{40}$ (0.1 mmol) was synthesized using a previously reported method[45] and dissolved in distilled water, while the viologen-based ionic liquid ($C_n$bpy·Br) (0.3 mmol) was dissolved in anhydrous ethanol. The ionic liquid solution was then added dropwise to the $H_3PMo_{12}O_{40}$ solution and stirred for 2 hours at room temperature. The resulting mixture was transferred to a hydrothermal synthesis reactor and heated at 80 °C for 12 hours. The yellow solid product was subsequently dried in a vacuum oven at 60 °C for 12 hours, yielding C_n–PMo_{12}. The successful synthesis of the products was confirmed by FT-IR, XRD, and SEM analyses (Fig. S6–S8).

2.2.3. Preparation for PDMS film. To improve operational convenience and expand the practical applications of these ionic liquids (ILs), C_6–PMo_{12} and C_{12}–PMo_{12} were utilized to fabricate composite membranes. Initially, C_6–PMo_{12} and C_{12}–PMo_{12} were ground into fine powders, which were then uniformly dispersed in dimethyl sulfoxide (DMSO) using ultrasonication. This dispersion was subsequently blended with polydimethylsiloxane (PDMS). The resulting mixture was applied to 200 μm films onto a glass substrate using a film applicator and cured in an oven at 80 °C. This process resulted in uniform composite films, which were labeled as C_6–PMo_{12}-a and C_{12}–PMo_{12}-b, respectively.

3. Results and discussion

3.1. Photochromic properties

The photochromic properties of the five ionic liquids (ILs) were studied by irradiating them with a Xe lamp. As shown in Fig. 2a, the color of C_3–PMo_{12} and C_4–PMo_{12} exhibited slight changes after 180 s of exposure. In contrast, C_5–PMo_{12} and C_6–PMo_{12} showed significant color changes within 10 s of irradiation. Notably, C_{12}–PMo_{12} displayed a quick response, transitioning from light yellow to light green in just 5 s. Both C_6–PMo_{12} and C_{12}–PMo_{12} reached a color saturation (deep olive green) after 10

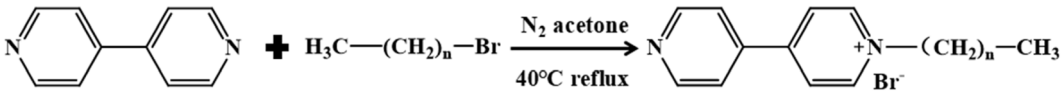

Fig. 1 Synthetic routes of viologen-based ionic liquids.

minutes of irradiation. The CIE1931 chromatic diagrams, derived from the L^*, a^*, b^* values of C_3–PMo_{12}, C_6–PMo_{12} (Fig. S9), and C_{12}–PMo_{12} (Fig. 2b) before and after 10 min irradiation, clearly demonstrate that C_{12}–PMo_{12} displays the most prominent color changes. The calculated color difference values ∇E of C_3–PMo_{12}, C_6–PMo_{12}, and C_{12}–PMo_{12} are 29.260, 72.360, and 85.040, respectively (Table S1). These values further confirm the high contrast and vivid photochromic behavior of C_{12}–PMo_{12}. As the alkyl chain length of the viologen-based cation increased, the coloring rate accelerated, and the color contrast enhanced, likely due to the suppression of viologen radical quenching by longer carbon chains. This remarkable photochromic response highlights the potential of C_{12}–PMo_{12} as a candidate for dynamic optical applications that require high-visibility color switching under Xe lamp excitation.

The photochromic behavior of the five ILs was investigated using UV-vis absorption spectroscopy. As shown in Fig. 3a and b, and the SI (Fig. S10), none of the five ILs exhibited significant absorption peaks in the 500–800 nm range before UV irradiation. However, upon exposure to UV light, a new broad absorption peak appeared within the 600–750 nm range, characteristic of viologen radicals.[46] Notably, the intensity of this absorption peak increased progressively with prolonged irradiation, indicating a gradual rise in the concentration of viologen radicals. These results suggest that the observed color change in these compounds is due to the light-induced formation of viologen radicals. Additionally, when UV-irradiated C_6–PMo_{12} and C_{12}–PMo_{12} were exposed to an H_2O_2 atmosphere for 3 hours, both compounds decolorized and returned to their original color. Upon reirradiation, the samples displayed a dark green coloration again, confirming that the photochromic properties of the ILs are reversible (Fig. S11). As illustrated in Fig. 3c and d, the coloration–decoloration cycling tests of C_6–PMo_{12} and C_{12}–PMo_{12} were performed over five cycles. It was found that the absorbance at 728 nm and 717 nm remained nearly unchanged for both C_6–PMo_{12} and C_{12}–PMo_{12}, demonstrating excellent photochromic reversibility and fatigue resistance.

To further assess the photochromic performance, detailed kinetic studies of C_6–PMo_{12} and C_{12}–PMo_{12} were conducted. The kinetic calculation equation used in this study is provided below:

$$\ln[(A_0 - A_\infty/A_t - A_\infty] = kt$$

Here, k is the rate constant, A_0 is the initial absorbance, A_t is the absorbance at time t, and A_∞ is the absorbance at photochemical saturation.[47]

In Fig. 3e and f, the rate constants derived from the absorption peaks at 728 nm and 717 nm indicate that both C_6–PMo_{12} and C_{12}–PMo_{12} follow a two-stage first-order kinetic behavior. The K_1 values for the initial stage are higher than the K_2 values for the second stage, suggesting that the primary photochromic process occurs on the surface at the beginning. As irradiation time increases, photochromic behavior progresses deeper into the material. Specifically, the K_1 and K_2 values for C_{12}–PMo_{12} are 0.0186 s^{-1} and 0.00784 s^{-1}, respectively, which are higher than those for C_6–PMo_{12}, with K_1 and K_2 values of 0.0158 s^{-1} and 0.00621 s^{-1}, respectively. These findings demonstrate that C_{12}–PMo_{12} exhibits a faster photochromic response compared to C_6–PMo_{12}.

3.2. Analysis of the photochromic mechanism

To investigate the photochromic mechanism, the electron paramagnetic resonance (EPR) of C_{12}–PMo_{12} was measured. As shown in Fig. 4a, C_{12}–PMo_{12} displayed a weak but detectable

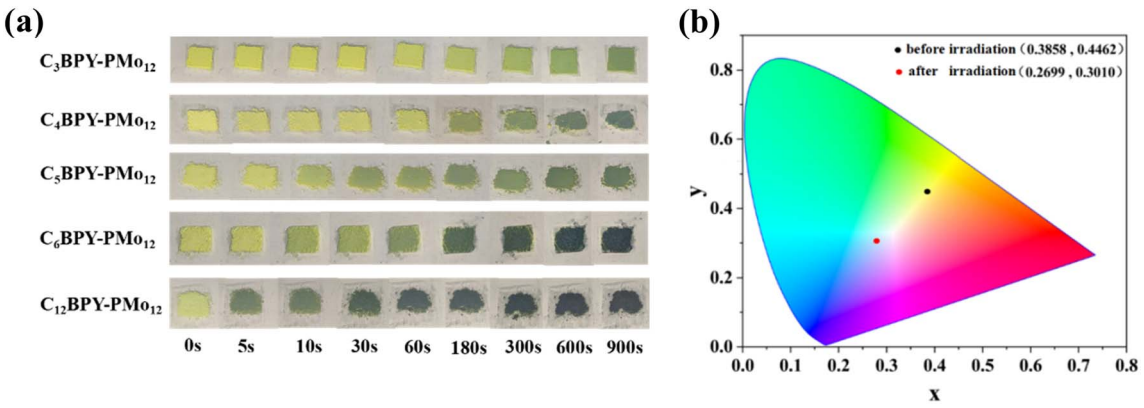

Fig. 2 (a) Photographs of the color change of the samples before and after irradiation with a Xe lamp. (b) CIE chromaticity diagrams of C_{12}–PMo_{12} before and after irradiation with a Xe lamp.

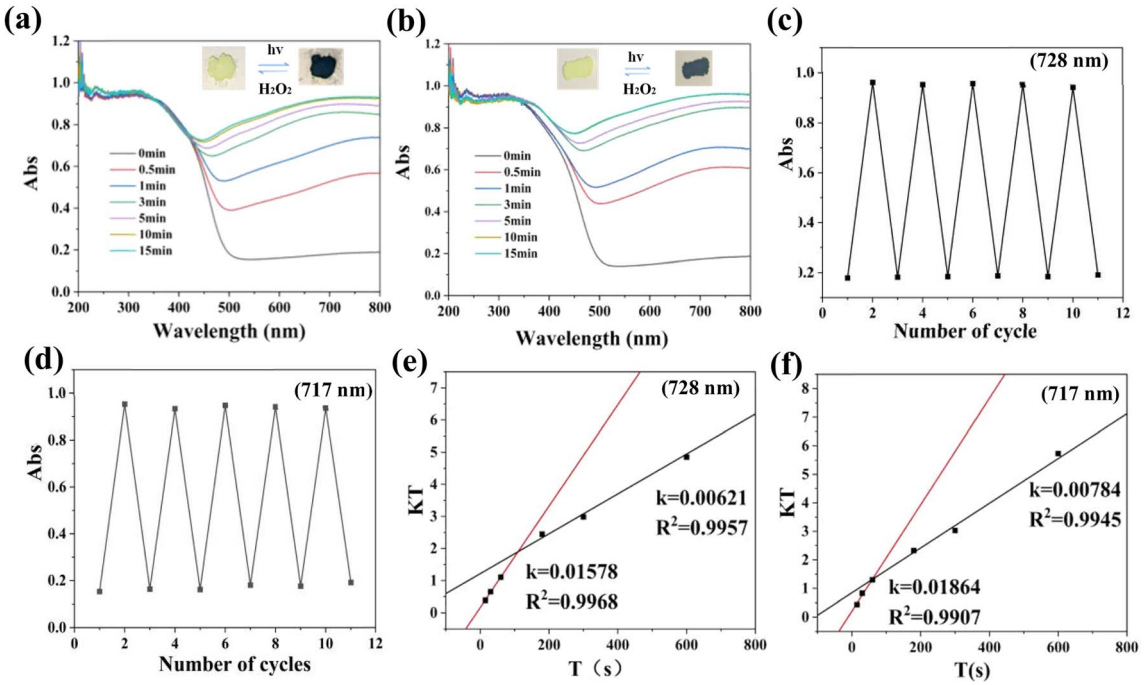

Fig. 3 (a and b) UV-vis absorption spectra of compound C_6–PMo_{12} (a), C_{12}–PMo_{12} (b) before and after irradiation with a Xe lamp. (c and d) UV-vis absorption value of the C_6–PMo_{12} at 728 nm (c) and C_{12}–PMo_{12} at 717 nm (d) according to photochromic repeatability. (e and f) Photochemical reaction kinetic plots monitored at 728 nm (e) and 717 nm (f).

EPR signal at $g = 2.0028$ before irradiation, which is attributed to trace viologen radical species.[48] This pre-existing signal indicates the intrinsic photosensitivity of the compound, as the viologen moiety exhibits partial electron activity even in the ground state. After irradiation, this signal was significantly enhanced. Furthermore, EPR analysis provided additional spectroscopic evidence of photoreduction, as a new signal appeared at $g = 1.9426$, characteristic of Mo(v) species formed by the partial reduction of Mo(vi) centers.[48] FT-IR and PXRD analyses were conducted on C_{12}–PMo_{12} before and after irradiation. The results showed that both the infrared spectrum (Fig. 4b) and the XRD (Fig. 4c) remained essentially unchanged, indicating that the structure and composition of C_{12}–PMo_{12} were unaffected by irradiation. After irradiation, the peak signal around 3500 cm^{-1} increased in intensity, which can be attributed to O–H stretching vibrations, possibly arising from trace amounts of water absorbed in the sample. In addition, a small peak appeared around 1200 cm^{-1}, which may correspond to the C–N stretching vibration in the reduced radical species. These findings suggest that the photochromic process involves reversible electron transfer without any structural reorganization.

The photochromic mechanism of C_{12}–PMo_{12} was further investigated using X-ray photoelectron spectroscopy (XPS). As shown in Fig. S12, the binding energies of C 1s and P 2p remained nearly unchanged before and after irradiation, indicating that these elements do not participate in the electron transfer process. However, significant changes were observed in the O 1s, N 1s, and Mo 3d spectra upon irradiation (Fig. 5). After exposure to UV light, the binding energy of O 1s (Fig. 5d)

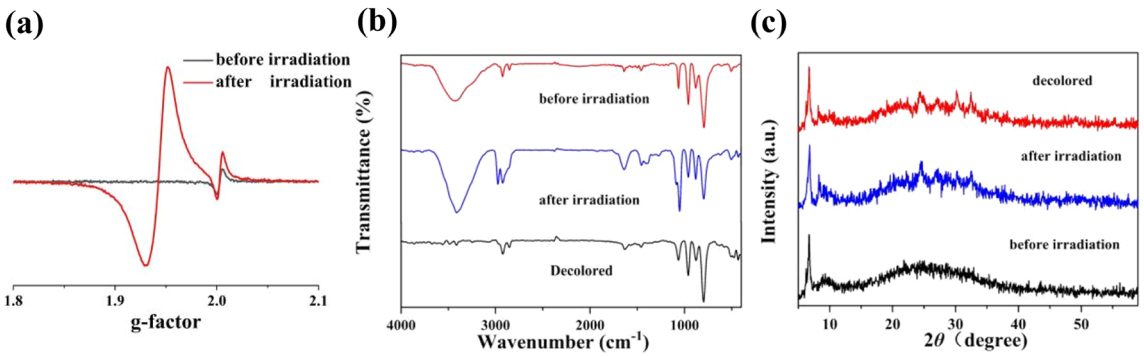

Fig. 4 (a and c) EPR, FT-IR, XRD spectra of C_{12}–PMo_{12} before and after irradiation.

increased compared to that before irradiation (Fig. 5a), suggesting that oxygen acts as an electron donor.[49] In contrast, the binding energy of N 1s slightly decreased (Fig. 5e), indicating that nitrogen functions as an electron acceptor. For the Mo 3d spectra (Fig. 5c), two prominent peaks at 232.45 eV and 235.54 eV were observed before irradiation, corresponding to Mo(VI). After light exposure (Fig. 5f), new peaks appeared at 233.16 eV and 236.24 eV. This suggests that electron transfer from $O_{Mo-O} \rightarrow Mo_{(IV)}$ and O_{POMS} to the viologen-based ionic liquids is responsible for the photochromism observed in C_{12}–PMo_{12}.

3.3. Applications

3.3.1. Inkless and erasable printing. The above results indicate that C_6–PMo_{12} and C_{12}–PMo_{12} exhibit excellent photochromic properties and reversibility, making them highly suitable for ink-free erasable printing applications. Consequently, these materials were further applied in this study for inkless erasable printing. The C_6–PMo_{12} and C_{12}–PMo_{12} powders were dispersed in ethanol through ultrasonic treatment for 30 minutes to create stable suspensions, which were then uniformly drop-cast onto filter paper[50] and dried, repeating the process three times. Upon exposure to a Xe lamp (Fig. 6a), distinct "HENU" patterns appeared within 15 seconds for C_6–PMo_{12} (Fig. S13) and 10 seconds for C_{12}–PMo_{12}. These patterns demonstrated substantial stability under ambient conditions, retaining their color for extended periods, thus offering advantages for long-term information storage. Moreover, the irradiated patterns could be erased in a controlled manner by placing the paper in a H_2O_2 atmosphere for 2 hours (C_6–PMo_{12}) and 1.5 hours (C_{12}–PMo_{12}). Repeating the printing and erasing process over five cycles (Fig. 6b) preserved the maximum contrast of the photochromic paper, demonstrating exceptional reversibility and durability. This is because the oxidation by H_2O_2 not only eliminates the radical but also completely removes their characteristic absorption band. Thus, even though the IL molecules remain on the filter paper, they are already in the colorless initial oxidized state and do not interfere with the coloration of the new patterns. These findings emphasize the potential of C_6–PMo_{12} and C_{12}–PMo_{12} as ink-free erasable printing materials, suitable for high-performance information storage and exchange applications.

3.3.2. UV light detection. Ultraviolet detectors are crucial for applications in environmental monitoring, medical diagnostics, and advanced security systems, enabling precise detection of UV radiation. In this work, flexible composite films based on C_6–PMo_{12} and C_{12}–PMo_{12} were designed and applied to UV photodetectors. The compounds C_6–PMo_{12} and C_{12}–PMo_{12} were homogeneously mixed with PDMS in DMSO and cast into uniform films using a film applicator, yielding membranes named C_6–PMo_{12}-a (Fig. 7a) and C_{12}–PMo_{12}-b (Fig. 7b), respectively. Upon irradiation with a Xe lamp for 2 min and 1.5 min, respectively, the C_6–PMo_{12}-a and C_{12}–PMo_{12}-b films exhibited a distinct color change from pale yellow-green to deep blue. Both membranes demonstrated excellent flexibility, being portable (Fig. 7c and d) and easily bendable without structural damage. Fig. 7e shows that these membranes also possess favorable mechanical properties, and the addition of C_6–PMo_{12} and C_{12}–PMo_{12} did not destroy the flexibility of the PDMS. UV-vis absorption spectra further confirmed that both C_6–PMo_{12}-a (Fig. 7f) and C_{12}–PMo_{12}-b (Fig. 7g) exhibited the

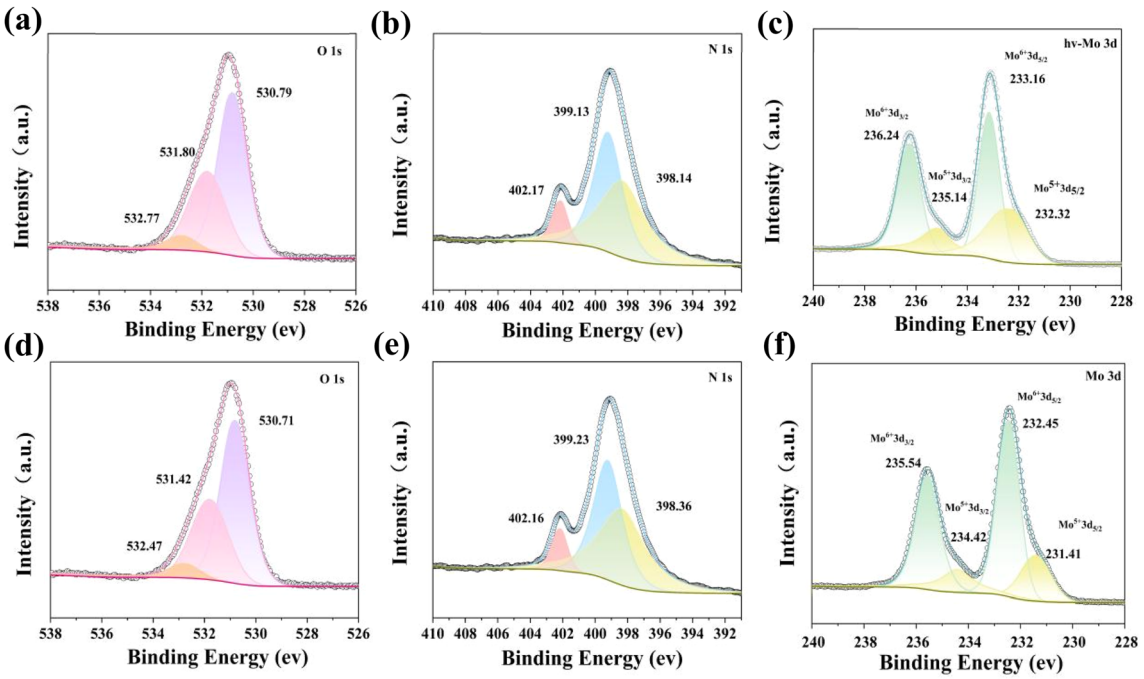

Fig. 5 (a–c) High resolution XPS spectra for C_{12}–PMo_{12} O 1s, N 1s, Mo 3d before irradiation. (d–f) High resolution XPS spectra for C_{12}–PMo_{12} O 1s, N 1s, Mo 3d after irradiation.

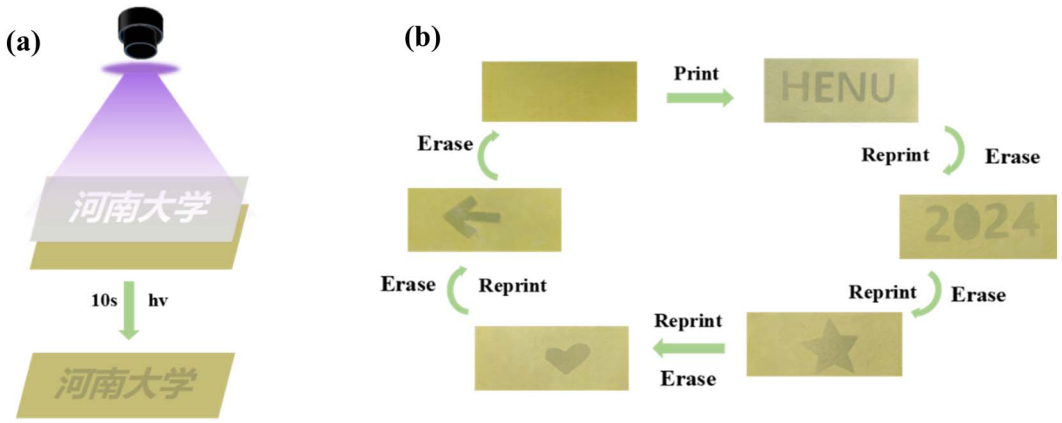

Fig. 6 (a) Schematic diagram of light printing. (b) Photos of samples in a cyclic light printing process.

appearance of new absorption bands in the 600–750 nm range after Xe lamp irradiation. The intensity of these absorption peaks increased systematically with prolonged exposure, consistent with the solid-state UV-vis absorption spectra. These results demonstrate that flexible membranes are easy to fabricate and operate, making them ideal for applications involving ultraviolet radiation monitoring.

3.3.3. Amine vapor detection. Organic amines are highly corrosive and toxic volatile compounds that pose significant risks to human health and contribute to air pollution. Consequently, the development of effective detection methods for organic amines and ammonia is essential.[51] To evaluate the detection performance of five ionic liquids (ILs) toward organic amines and ammonia, several representative organic amine compounds were selected, including ammonia (NH_3), diethylamine (DEA), *N*,*N*-dimethylformamide (DMF), and acetonitrile (CH_3CN). When these five ILs were exposed to ammonia vapor, distinct color changes were observed over time (Fig. S14). The color of C_6–PMo_{12} and C_{12}–PMo_{12} transitioned from yellow to off-white after 1.5 minutes in the NH_3 atmosphere (Fig. 8a) and reverted to yellow after 4 minutes in the HCl atmosphere (Fig. S15). C_3–PMo_{12}, C_4–PMo_{12}, and C_5–PMo_{12} also changed from yellow to white-gray within 3 minutes. Additionally, the colour of C_6–PMo_{12}-a and C_{12}–PMo_{12}-b shifted from light green to gray-white after 1.5 minutes in the NH_3 atmosphere, with recovery upon exposure to concentrated HCl for 4 minutes

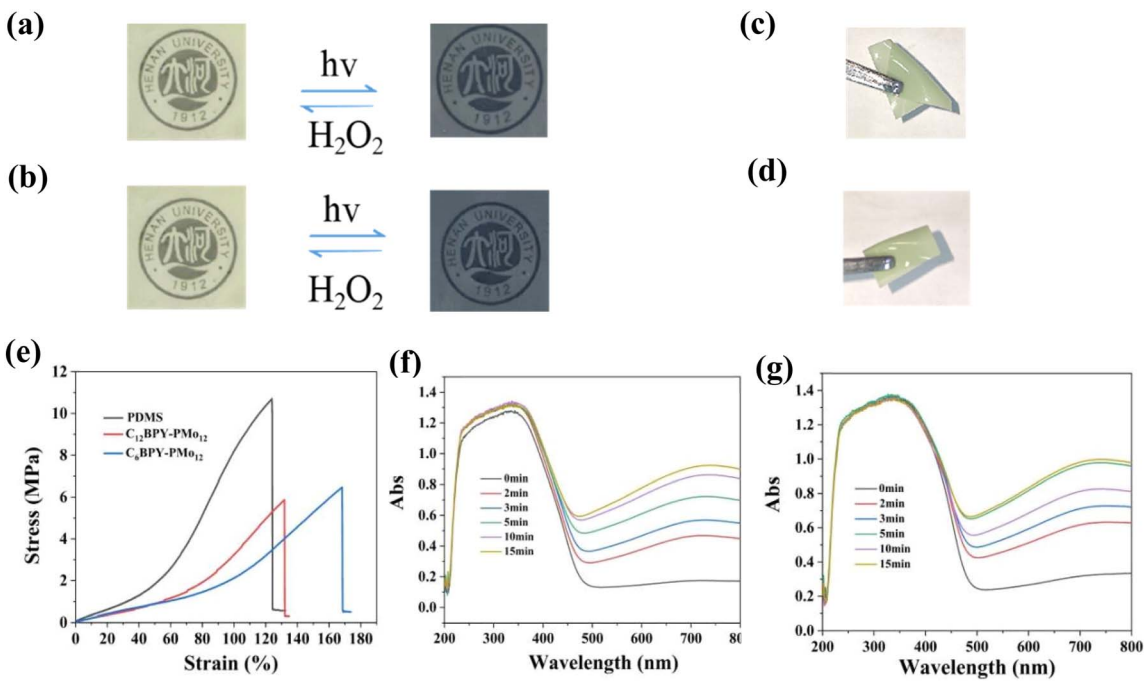

Fig. 7 (a and b) Color change of C_6–PMo_{12}-a and C_{12}–PMo_{12}-b before and after photochromism. (c and d) Flexibility of C_6–PMo_{12}-a and C_{12}–PMo_{12}-b. (e) Stress–strain curves of PDMS, C_6–PMo_{12}-a, and C_{12}–PMo_{12}-b. (f and g) The UV-vis spectra of compound C_6–PMo_{12}-a and C_{12}–PMo_{12}-b before and after irradiation with a Xe lamp.

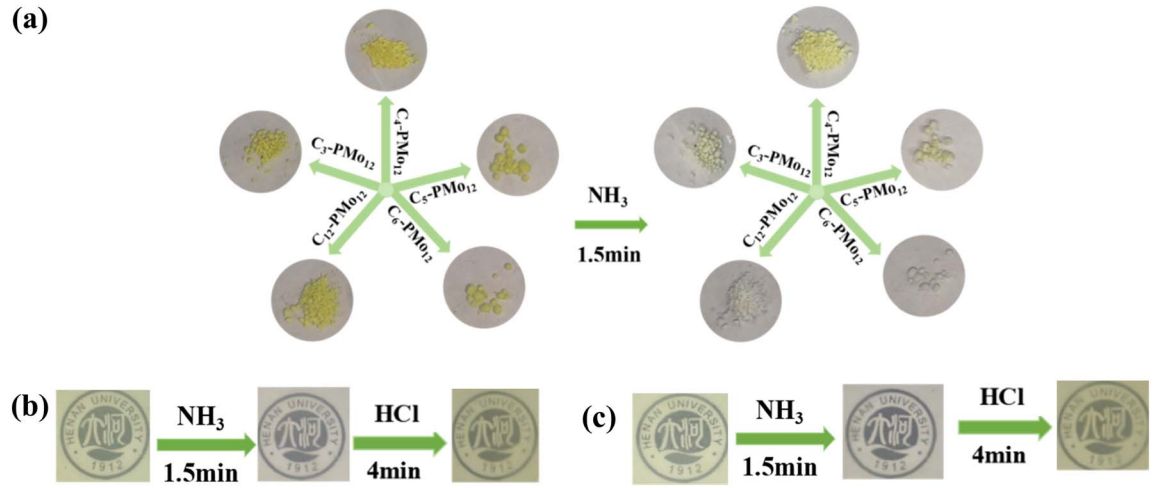

Fig. 8 (a) Color change of C_n–PMo_{12} before and after 1.5 min detection of NH_3. (b and c) Color change of C_6–PMo_{12}-a, C_{12}–PMo_{12}-b in HCl and organic amine.

(Fig. 8b and c). After three cycles of coloration and decoloration, the color contrast remained stable (Fig. S16). When C_{12}–PMo_{12} was placed in ammonia ($NH_3 \cdot H_2O$), *N*,*N*-dimethylformamide (DMF), diethanolamine (DEA), and acetonitrile (CH_3CN) atmospheres for 10 minutes, significant color changes were observed in $NH_3 \cdot H_2O$ and DEA, while minimal changes occurred in DMF and CH_3CN after 1 hour (Fig. S17). This behavior can be attributed to the relationship between the detection efficiency of the ionic liquid and the molecular size of the target amines. Smaller molecules, such as ammonia and primary amines, readily form hydrogen bonds with the ionic liquid, facilitating electron transfer and generating viologen free radicals. In contrast, bulkier secondary and tertiary amines introduce steric hindrance, which limits hydrogen bond formation and hinders electron transfer.[52] These results indicate that C_{12}–PMo_{12} demonstrates high selectivity for amine detection.

4. Conclusion

In this study, five polyoxometalate-based viologen ionic liquids (ILs) with various substituents were synthesized, each exhibiting outstanding multi-stimuli responsive capabilities. Among these, the IL with the longest alkyl chain, C_{12}–PMo_{12}, demonstrated the fastest coloration rate and highest color contrast, transitioning from light yellow to light green in just 5 seconds under xenon lamp irradiation, likely due to the suppression of viologen radical quenching by longer carbon chains. All the colored ILs were able to revert to their original state in an H_2O_2 atmosphere, with no change in color contrast after five cycles of coloration and decoloration, indicating exceptional fatigue resistance. These ionic liquids were further applied as photochromic layers for the fabrication of rewritable paper, among which C_{12}–PMo_{12} displayed clear and legible text within only 10 seconds. The printed text exhibited excellent stability, retaining its colored state for extended periods under ambient conditions, thereby demonstrating suitability for long-term information storage. Remarkably, the written content could be fully erased within 1.5 hours in an H_2O_2 atmosphere, highlighting the potential of these materials for inkless and erasable printing. In addition, flexible composite membranes incorporating these ILs were fabricated, showing promising performance as portable UV photodetectors. These compounds also exhibited pronounced and highly selective responses toward organic amines. Overall, this work broaden the application range of polyoxometalate–viologen ILs, providing theoretical insights for their future applications in photochromism, UV detection, and organic amine monitoring.

Conflicts of interest

The authors declare that they have no known competing financial interests or personal relationships that could have appeared to influence the work reported in this paper.

Data availability

The data supporting this article have been included as part of the supplementary information (SI). Supplementary information: including 1H NMR, FT-IR, XRD and SEM data of these five ILs; CIE chromaticity diagrams of C3-PMo12, C6-PMo12; color change of C_n-PMo_{12} with UV light, amine; and so on. See DOI: **https://doi.org/10.1039/d5ra05884h**.

Acknowledgements

This work was supported by the National Natural Science Foundation of China (22408084), Young Elite Scientists Sponsorship Program by CAST (2022QNRC001) and Henan Provincial Science and Technology Research Project (242102231082).

References

1 A. Abdollahi, H. Roghani-Mamaqani and B. Razavi, Stimuli-chromism of photoswitches in smart polymers: recent

advances and applications as chemosensors, *Prog. Polym. Sci.*, 2019, **98**, 101149–101210, DOI: **10.1016/j.progpolymsci.2019.101149**.

2 A. Samanta, H. Chen, P. Samanta, S. Popov, I. Sychugov and L. Berglund, Reversible Dual-Stimuli-Responsive Chromic Transparent Wood Biocomposites for Smart Window Applications, *ACS Appl. Mater. Interfaces*, 2021, **13**, 3270–3277, DOI: **10.1021/acsami.0c21369**.

3 Z. Yang, L. Chen, D. J. McClements, C. Qiu, C. Li, Z. Zhang, M. Miao, Y. Tian, K. Zhu and Z. Jin, Stimulus-responsive hydrogels in food science: a review, *Food Hydrocoll.*, 2022, **124**, 107218–107230, DOI: **10.1016/j.foodhyd.2021.107218**.

4 Y. Y. Lin, C. J. Jiao, Y. G. Qi, J. W. Zou, D. H. Xu and S. F Luan, Multiple Stimuli-Responsive Color-Changing Polymer Materials for Reversible Writing and Anti-Counterfeiting, *ACS Appl. Mater. Interfaces*, 2024, **16**, 43064–43071, DOI: **10.1021/acsami.4c10488**.

5 X. Wang, R. Lin, W. Sun, J. Liu, L. Xu, C. Redshaw and X. Feng, Cucurbit [7] Uril-Based Self-Assembled Supramolecular Complex with Reversible Multistimuli-Responsive Chromic Behavior and Controllable Fluorescence, *Adv. Opt. Mater.*, 2024, **12**, 2400839–2400848, DOI: **10.1002/adom.202400839**.

6 C. Wang, R. Huo, F. Xu, Y. Xing and F. Bai, Multiple stimulus responsive Co-AIE framework materials with reversible solvatochromic and thermochromic behaviors: molecular design, synthesis and characterization, *J. Mater. Chem. C*, 2022, **10**, 17723–17733, DOI: **10.1039/d2tc03819f**.

7 T. Chen, Q. Yang, C. Fang, S. Deng and B. Xu, Advanced Design for Stimuli-Reversible Chromic Wearables With Customizable Functionalities, *Adv. Mater.*, 2024, **37**, e2413665, DOI: **10.1002/adma.202413665**.

8 X. Wang, C. Xu, R. Lin, W. Sun, M. Ye, L. Xu and J. Liu, Acid-base regulated inclusion complexes of β-cyclodextrin with 1-[2-(4-fluorophenyl)-2-oxoethyl]-4,4′-bipyridinium dichloride displaying multistimuli-responsive chromic behaviors and photomodulable fluorescence, *J. Mater. Chem. C*, 2024, **12**, 2764–2771, DOI: **10.1039/d3tc04555b**.

9 T. Saleh, G. Fadillah and E. Ciptawati, Smart advanced responsive materials, synthesis methods and classifications: from Lab to applications, *J. Polym. Res.*, 2021, **28**, 197–212, DOI: **10.1007/s10965-021-02541-x**.

10 C. Zhu, L. Zhang, A. Zou, W. Wang, J. Zhang and A. Zhang, A bionic intelligent hydrogel with multi-level information encryption and decryption capabilities, *Chem. Eng. J.*, 2023, **475**, 146161–14672, DOI: **10.1016/j.cej.2023.146161**.

11 X. Yuan, J. Wang, Y. Li, H. Huang, J. Wang, T. Shi, Y. Deng, Q. Yuan, R. He, P. Chu and X. Yu, Multilevel Information Encryption Based on Thermochromic Perovskite Microcapsules via Orthogonal Photic and Thermal Stimuli Responses, *ACS Nano*, 2024, **18**, 10874–10884, DOI: **10.1021/acsnano.4c00938**.

12 D. Zhang, B. Ren, Y. Zhang, L. Xu, Q. Huang, Y. He, X. Li, J. Wu, J. Yang, Q. Chen, Y. Chang and J. Zheng, From design to applications of stimuli-responsive hydrogel strain sensors, *J. Mater. Chem. B*, 2020, **8**, 3171–3191, DOI: **10.1039/c9tb02692d**.

13 F. Alam, M. Elsherif, A. Salih and H. Butt, 3D printed polymer composite optical fiber for sensing applications, *Addit. Manuf.*, 2022, **58**, 102996–103018, DOI: **10.1016/j.addma.2022.102996**.

14 J. Wang, Z. Zhou, X. Li and C. Chang, Cellulose nanocrystals-based optical organohydrogel fiber with customizable iridescent colors for strain and humidity response, *Int. J. Biol. Macromol.*, 2024, **275**, 133501–133508, DOI: **10.1016/j.ijbiomac.2024.133501**.

15 O. Anitha, M. Mathivanan, B. Tharmalingam, T. Thiruppathiraja, S. Ghorai, R. Natarajan, V. Thiagarajan, S. Lakshmipathi and B. Murugesapandian, Multi-stimuli responsiveness of pyrimidine bishydrazone: AIE, tuneable luminescence, white light emission, mechanochromism, acidochromism and its anticounterfeiting applications, *Dyes Pigm.*, 2023, **212**, 111091–111103, DOI: **10.1016/j.dyepig.2023.111091**.

16 S. Zhao, A. Yuan, X. Chen, Y. Lei, X. Fu, J. Lei and L. Jiang, Single-actuated and fully recyclable phase change materials enabled multiple thermochromism toward information storage and encryption, *Chem. Eng. J.*, 2024, **481**, 148698–148708, DOI: **10.1016/j.cej.2024.148698**.

17 Z. Guo, Y. Su, H. Zong, F. Zhou, M. Wang and G. Zhou, A Universal Strategy for Reversible Photochromism of Viologen Derivatives in Solutions, *Adv. Opt. Mater.*, 2024, **12**, 2401791–2401800, DOI: **10.1002/adom.202401791**.

18 Y. Luo, J. Liu, L. Li and S. Zang, Multi-Stimuli-Responsive Chromic Behaviors of an All-in-One Viologen-Based Cd (II) Complex, *Inorg. Chem.*, 2023, **62**, 14385–14392, DOI: **10.1021/acs.inorgchem.3c02070**.

19 X. Zhang, Z. Wang, X. Huang, Q. Huang, Y. Wen, B. Li, M. Holmes, J. Shi and X. Zou, Uniform stain pattern of robust MOF-mediated probe for flexible paper-based colorimetric sensing toward environmental pesticide exposure, *Chem. Eng. J.*, 2023, **451**, 138928–138938, DOI: **10.1016/j.cej.2022.138928**.

20 P. He and B. Derby, Controlling Coffee Ring Formation during Drying of Inkjet Printed 2D Inks, *Adv. Mater. Interfaces*, 2017, **4**, 1700944–1700950, DOI: **10.1002/admi.201700944**.

21 J. Liu, Multi-responsive host-guest MOFs derived from ethyl viologen cations, *Dyes Pigm.*, 2019, **163**, 496–501, DOI: **10.1016/j.dyepig.2018.12.033**.

22 B. Tan, C. Chen, L. Cai, Y. Zhang, X. Huang and J. Zhang, Introduction of lewis acidic and redox-active sites into a porous framework for ammonia capture with visual color response, *Inorg. Chem.*, 2015, **54**, 3456–3461, DOI: **10.1021/acs.inorgchem.5b00023**.

23 J. Zhang, Y. Zeng, H. Lu, X. Chen, X. Yuan and Z. Fu, Two Zinc-Viologen Interpenetrating Frameworks with Straight and Offset Stacking Modes Respectively Showing Different Photo/Thermal Responsive Characters, *Cryst. Growth Des.*, 2020, **20**, 2617–2622, DOI: **10.1021/acs.cgd.9b01736**.

24 Z. Huang, L. Zhang and H. Sun, Step-wise assembly of a dysprosium-viologen framework with photoswitchable slow magnetic relaxation under a zero dc field, *Inorg. Chem. Front.*, 2025, **12**, 515–523, DOI: **10.1039/d4qi02771j**.

25 K. Li, T. Liu, J. Ying, A. Tian and X. Wang, A POM/viologen-based supramolecular fluorescent probe for Ag^{+} detection and application of visible hydrogel based intelligent sensing system, *Dyes Pigm.*, 2024, **222**, 111898–111907, DOI: 10.1016/j.dyepig.2023.111898.

26 H.-Y. Li, X. Hua, T. Fu, X.-F. Liu and S.-Q. Zang, Photochromic and electrochromic properties of a viologen-based multifunctional Cd-MOF, *Chem. Commun.*, 2022, **58**, 7753–7756, DOI: 10.1039/d2cc02703h.

27 S. Hu, J. Zhang, S. Chen, J. Dai and Z. Fu, Efficient Ultraviolet Light Detector Based on a Crystalline Viologen-Based Metal-Organic Framework with Rapid Visible Color Change under Irradiation, *ACS Appl. Mater. Interfaces*, 2017, **9**, 39926–39929, DOI: 10.1021/acsami.7b13367.

28 M. Li, X. Li, L. Huang, R. Song, J. Yang and H. Zhang, A novel photochromic complex based on a viologen ligand with rapid inkless and erasable printing, anti-counterfeiting and amine-selective responses, *Inorg. Chem. Commun.*, 2023, **153**, 110839–110845, DOI: 10.1016/j.inoche.2023.110839.

29 P. Liu, T. Liu, X. Shen and J. Liu, A new photochromic Mg(II)-viologen complex with photoswitchable emission and its application in ink-free printing, *Z. Anorg. Allg. Chem.*, 2023, **649**, e202300159, DOI: 10.1002/zaac.202300159.

30 D. Yang, T. Xiao, Y. Yang, J. Xue, Y. Shi, Q. Ma and X. Zheng, Two viologen-based complexes as persistent luminescent materials and their applications in inkless print and anticounterfeiting, *Chem. Eng. J.*, 2024, **488**, 151047–151056, DOI: 10.1016/j.cej.2024.151047.

31 Y. Yang, G. Wang, K. Li, W. Yang, J. Zhang, J. Zhang, S. Li and X. Zhang, Tuning up of chromism, luminescence in cadmium-viologen complexes through polymorphism strategy: Inkless erasable printing application, *Chin. Chem. Lett.*, 2025, **36**, 110123–110127, DOI: 10.1016/j.cclet.2024.110123.

32 T. Sagara and H. Tahara, Redox of Viologen for Powering and Coloring, *Chem. Rec.*, 2021, **21**(9), 2375–2388, DOI: 10.1002/tcr.202100082.

33 P. Wang, C. Yu, X. Yu, M. Wang and G. Guo, UV-vis/X-ray/thermo-induced synthesis and UV-SWIR photoresponsive property of a mixed-valence viologen molybdate semiconductor, *Chem. Commun.*, 2021, **57**, 5550–5553, DOI: 10.1039/d1cc00614b.

34 Q. Lu, A. Tian, S. Yu, X. Xu, S. Ma and M. Yang, Four Polyoxometalate-Viologen Discoloration Materials for UV Probing, Inkless and Erasable Printing and Visual Detection of Hg^{2+}, *Eur. J. Inorg. Chem.*, 2022, **26**, e202200672, DOI: 10.1002/ejic.202200672.

35 Q. Lu, J. Ying, A. Tian and X. Wang, A Series of POM-Viologen Photo-/Electrochromic Hybrids and Hydrogels Acting as Multifunctional Sensors for Detecting UV, Hg(2+), and Organic Amines, *Inorg. Chem.*, 2023, **62**, 16617–16626, DOI: 10.1021/acs.inorgchem.3c02743.

36 X. Wu, Q. Fan, Z. Bai, Q. Zhang, W. Jiang, Y. Li, C. Hou, K. Li and H. Wang, Synergistic Interaction of Dual-Polymer Networks Containing Viologens-Anchored Poly(ionic liquid)s Enabling Long-Life and Large-Area Electrochromic Organogels, *Small*, 2023, **19**, e2301742, DOI: 10.1002/smll.202301742.

37 S. Yu, T. Liu, J. Ying, A. Tian, M. Yang and X. Wang, A series of isopolymolybdate-viologen hybrids with photo-, thermo- and electro-chromic properties, *Dalton Trans.*, 2023, **52**, 16631–16639, DOI: 10.1039/d3dt02928j.

38 S. Yu, A. Tian, Q. Lu, X. Xu, S. Ma, X. Wang and Z. Wang, Polyoxometalate-Viologen Thermochromic Hybrids for Organic Amine Detectors and Memristors with Temperature-Regulating Resistance Switching Characteristics, *Inorg. Chem.*, 2023, **62**, 1549–1560, DOI: 10.1021/acs.inorgchem.2c03746.

39 Y. Gong, T. Liu, M. Yang, A. Tian and J. Ying, A series of viologen/POM materials with discoloration properties under the stimulation of X-ray, UV, electricity, and organic amines, *Spectrochim. Acta, Part A*, 2024, **313**, 124154–124161, DOI: 10.1016/j.saa.2024.124154.

40 L. Li, Y. Zou, Y. Hua, X. Li, Z. Wang and H. Zhang, Polyoxometalate-viologen photochromic hybrids for rapid solar ultraviolet light detection, photoluminescence-based UV probing and inkless and erasable printing, *Dalton Trans.*, 2020, **49**, 89–94, DOI: 10.1039/c9dt04116h.

41 X. Xu, M. Yang, Q. Lu, S. Yu, S. Ma, A. Tian and J. Ying, Three photochromic materials based on POMs and viologens for UV probing, visual detection of metal ions and amine detection, *CrystEngComm*, 2022, **24**, 7677–7685, DOI: 10.1039/d2ce01244h.

42 B. Chen, Y. Huang, K. Song, X. Lin, H. Li and Z. Chen, Molecular Nonvolatile Memory Based on $[\alpha\text{-}GeW_{12}O_{40}]^{4-}$/Metalloviologen Hybrids Can Work at High Temperature Monitored by Chromism, *Chem. Mater.*, 2021, **33**, 2178–2186, DOI: 10.1021/acs.chemmater.1c00090.

43 G. Chen, L. Zhang, Y. Zhang, K. Liu, Z. Long and Y. Wang, Targeted synthesis of ionic liquid-polyoxometalate derived Mo-based electrodes for advanced electrochemical performance, *J. Mater. Chem. A*, 2019, **7**, 7194–7201, DOI: 10.1039/c8ta12562g.

44 K. Madasamy, D. Velayutham, V. Suryanarayanan, M. Kathiresan and K. Ho, Viologen-based electrochromic materials and devices, *J. Mater. Chem. C*, 2019, **7**, 4622–4637, DOI: 10.1039/c9tc00416e.

45 X. Xu, M. Xie, K. Xu and Y. Zhao, g-C_3N_4@PMo_{12} composite material double adjustment improves the performance of perovskite-based photovoltaic devices, *Sol. Energy*, 2020, **209**, 363–370, DOI: 10.1016/j.solener.2020.08.095.

46 C. Zhang, H. Shi, Y. Yan, L. Sun, Y. Ye, Y. Lu, Z. Liang and J. Li, A zwitterionic ligand-based water-stable metal-organic framework showing photochromic and Cr(vi) removal properties, *Dalton Trans.*, 2020, **49**, 10613–10620, DOI: 10.1039/c9dt04679h.

47 G. Li, J. Zhang, W. Ren, S. Wang, Y. Wang, Y. Fu and Y. Wang, Electron density effect of aromatic carboxylic acids in naphthalenediimide-based coordination polymers: from thermal electron transfer and charge transfer to photoinduced electron transfer, *Dalton Trans.*, 2023, **52**, 16184–16188, DOI: 10.1039/d3dt03069e.

48 J. Ying, L. Jin, C. Sun, A. Tian and X. Wang, A Series of Polyoxometalate-Viologen Photochromic Materials for UV Probing, Amine Detecting and Inkless and Erasable Printing, *Chem.–Eur. J.*, 2021, **28**, e202103268, DOI: **10.1002/chem.202103268**.

49 H. Wang, Z. Tu and H. Zhang, A novel photochromic coordination polymer based on a robust viologen ligand exhibiting multiple detection properties in the solid state, *Dalton Trans.*, 2019, **48**, 17852–17857, DOI: **10.1039/c9dt03835c**.

50 Y. Liu, M. Li, Q. Zhao, H. Wu, K. Huang and F. Li, Phosphorescent iridium(III) complex with an N;O ligand as a Hg(2+)-selective chemodosimeter and logic gate, *Inorg. Chem.*, 2011, **50**, 5969–5977, DOI: **10.1021/ic102481x**.

51 B. Garai, A. Mallick and R. Banerjee, Photochromic metal-organic frameworks for inkless and erasable printing, *Chem. Sci.*, 2016, **7**, 2195–2200, DOI: **10.1039/c5sc04450b**.

52 X. Hao, T. Liu, Y. Li, J. Ying, A. Tian, M. Yang and X. Wang, Four POM-viologen color-changing materials with fast color response under various external stimuli, *Inorg. Chem.*, 2024, **63**, 5852–5864, DOI: **10.1021/acs.inorgchem.3c04282**.